Available online at www.sciencedirect.com
ScienceDirect
Cement & Concrete Composites 29 (2007) 94–102
Cement & Concrete Composites
www.elsevier.com/locate/cemconcomp

Influence of limestone powder used as filler in SCC on hydration and microstructure of cement pastes

G. Ye [a,b,*], X. Liu [c], G. De Schutter [a], A.-M. Poppe [a], L. Taerwe [a]

[a] Magnel Laboratory for Concrete Research, Department of Structural Engineering, Ghent University, Technologiepark-Zwijnaarde 904 B-9052, Ghent (Zwijnaarde), Belgium
[b] Microlab, Faculty of Civil Engineering and Geosciences, Delft University of Technology, Delft, The Netherlands
[c] School of Civil Engineering, Tongji University, Shanghai, China

Received 22 November 2005; received in revised form 29 August 2006; accepted 22 September 2006
Available online 14 November 2006

Abstract

In recent years, self-compacting concrete (SCC) has gained wide application in the construction industry. As for high performance concrete (HPC) and traditional concrete (TC), the microstructural properties of SCC are the main factors, which determine the material properties, i.e. the mechanical properties, transport properties and the durability behaviour.

In order to investigate the development of the microstructure of SCC, the microstructural parameters of the paste including porosity, pore size distribution and phase distribution are determined by means of mercury intrusion porosimetry (MIP) and scanning electron microscopy (SEM). The thermogravimetric analysis (TGA) and the derivative thermogravimetric analysis (DTG) are used to identify the phase constituents. These parameters as studied for self-compacting concrete are compared with high performance concrete and traditional concrete. The specimens of self-compacting cement paste (SCCP) are made with water/binder ratio 0.41 and 0.48, the high performance cement paste (HPCP) with w/c 0.33 and traditional cement paste (TCP) with w/c 0.48. The measurements are performed at different hydration stages, i.e. at 1, 3, 7, 14, 28 and 56 days.

The result of this research shows that the pore structure, including the total pore volume, pore size distribution and critical pore diameter, in the SCCP is very similar to that of HPCP. The fact that limestone powder does not participate in the chemical reaction was confirmed both from thermal analysis and BSE image analysis.

Keywords: Self compacting cement paste; Filler; Hydration; Microstructure; SEM

1. Introduction

Self-compacting concrete (SCC) is defined as a highly flowable, yet stable concrete that can spread readily into place and fill the formwork without any consolidation and without undergoing any significant segregation [1,2]. It was developed about 15 years ago [3,4] in Japan and since then it has received wide use in the construction industry [5].

Since the birth of SCC, most investigations have mainly concentrated on the influence of various admixtures [6,7] on hydration, on mix design [8–10] and on workability [11–14]. In general, self-compacting concrete consists basically of the same components as traditional concrete (TC) and as high performance concrete (HPC). However, due to the high filler content, i.e. limestone powder or fly ash, the microstructural aspects may be different.

From previous studies on high performance concrete and traditional concrete, it appears that the microstructural properties are the main factors which determine the

* Corresponding author. Address: Microlab, Faculty of Civil Engineering and Geosciences, Delft University of Technology, Delft, The Netherlands. Tel.: +31 15 2784001; fax: +31 15 2786383.
E-mail address: ye.guang@citg.tudelft.nl (G. Ye).

0958-9465/$ - see front matter © 2006 Elsevier Ltd. All rights reserved.
doi:10.1016/j.cemconcomp.2006.09.003

material characteristics, i.e. the mechanical properties, transport properties and the durability behaviour. In this context the aim of this study is to verify whether the properties of hardening/hardened self-compacting concrete, high performance and traditional concrete are influenced in a different way by the microstructural properties, especially, when the high content of limestone powder was added as filler.

It has to be mentioned that, in order to avoid the influence of aggregates on the microstructure, in this study only the cement pastes of SCC, HPC and TC were investigated. All specimens were made with the same mix proportion as for the concrete, however without any aggregate.

For clarification of these questions, various pastes were evaluated regarding the microstructural properties, i.e. porosity, pore size distribution and phase distribution. To this end, mercury intrusion porosimetry measurements (MIP) have been performed on self-compacting cement paste (SCCP), high performance cement pastes (HPCP) and traditional cement pastes (TCP) at different curing ages. And scanning electron microscopy (SEM) was employed to examine the phase distribution (CSH, $Ca(OH)_2$, unhydrated cement core and filler). The thermogravimetric analysis (TGA) and the derivative thermogravimetric analysis (DTG) were used to identify the phase constituents. The results were compared with each other.

2. Materials and methods

2.1. Materials

The mixtures used in this study were prepared with Portland cement CEM I 52.5. Limestone powder, produced from carboniferous limestone of a very high purity (98% of $CaCO_3$ content), was added as filler. The density of limestone powder was 2650 kg/m^3. The chemical properties of the cement and limestone powder used are presented in Table 1.

Table 1
The chemical and physical properties of cement and limestone powder

	CEM I 52.5 (%)	Limestone filler (%)
CaO	63.95	–
SiO_2	20.29	0.80
Al_2O_3	4.52	0.17
Fe_2O_3	2.35	0.10
MgO	2.22	0.50
K_2O	0.94	–
Na_2O	0.20	–
SO_3	3.35	–
Cl^-	0.015	0.002
$CaCO_3$	–	98.00
C_3S	59.0	–
C_2S	12.60	–
C_3A	8.01	–
C_4AF	9.40	–

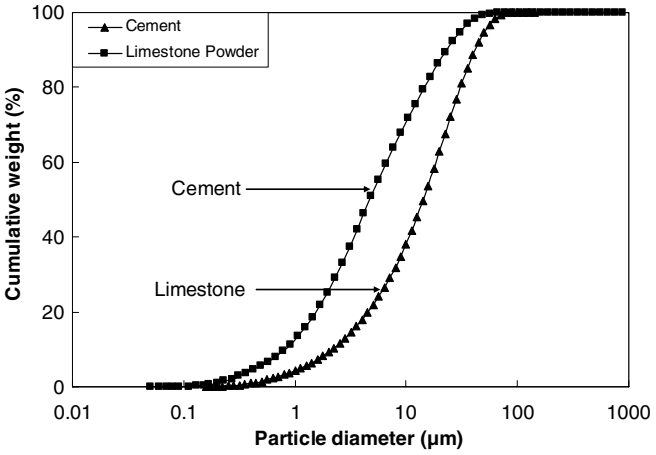

Fig. 1. Particle size distribution of cement and limestone.

In Fig. 1, the particle size distribution of Portland cement and limestone powder measured by laser diffraction are shown. The Blaine values of the limestone powder and CEM I 52.5 are 526 m^2/kg and 420 m^2/kg, respectively. The average particle size of the limestone filler is slightly smaller than that of the Portland cement CEM I 52.5.

2.2. Mixture design and specimen casting

The mix proportions of SCCP, HPCP and TCP are listed in Table 2.

First, the cement was mixed with water for 2 min at low speed. Afterwards, the superplasticizer was added and the paste was mixed for another 3 min at high speed. After mixing, the cement pastes were immediately cast into 1000 ml plastic bottles. The HPCP and TC samples were compacted with a shaking table in 2 min. The bottles were full filled paste before sealed. After shaking, the plastic bottles were rotated at a speed of 5 rpm in a room at a temperature of 20 °C. After 24 h of rotation, the samples were still kept in the plastic bottle and stored in the curing room at a temperature of 20 °C and relative humility 60% until the age of testing. These rotational procedures avoid the influence of bleeding on the pore structure in cement paste [15]. At different ages, the samples were split from the plastic bottle and were dried in an oven at 105 °C for 24 h till constant weight.

Table 2
Mix properties of cement paste (in kg, unless stated otherwise)

	TCP	SCCP1	SCCP2	HPCP
Portland cement I 52.5	350	400	400	400
Water	165	165	192	132
Limestone powder	–	200	300	–
Glenium 51 (l)	–	3.2	2.7	–
Superplasticizer Rheobuild	–	–	–	8.45
Total powder content		600	700	400
Water/cement ratio	0.48	0.41	0.48	0.33
Water/powder ratio	0.48	0.28	0.27	0.33

2.3. Thermometric isothermal calorimeter measurements

The rates of heat evolution of all pastes were measured in a thermometric isothermal conduction calorimeter (TEM Air 314), using 10 g samples. All measurements were performed at a temperature of 20 °C.

2.4. Mercury intrusion porosimetry measurements

MIP is used to determine the pore size distribution of pastes. Although numerous researchers have reported the limitations of MIP for the determination of the pore structure of cementitious materials [16], however MIP is so far the most widely used method for this. As pointed out by Diamond [16], this is not because it "fits" the system best, but because it is the only available procedure that purports to cover nearly the whole range of sizes that must be tallied.

The measurements were made with a PMI automated porosimeter with a maximum pressure of 420 MPa. In order to avoid damage of the CSH gel structure at high pressures, the highest pressure used in the experiments was 212 MPa. According to the Washburn equation [17], with this pressure a minimum pore diameter of 0.0069 μm can be accessed.

2.5. BSE image acquisition and analysis

Scanning electron microscopy was used to determine the microstructure and the phase distribution of the samples. In order to obtain high quality images using a backscattering scanning electron detector, the samples have to be prepared carefully, including epoxy impregnation, cutting, grinding and polishing. The procedure has been described in [15].

The images were obtained in water vapour mode. In order to get a high contrast image for image analysis, an acceleration voltage around 20 kV was used. The physical size of the region in each image is 263 μm in length and 186 μm in width when a magnification factor of 500 was used. The image size is 1728×1027 pixels, so the resolution is 0.152 μm per pixel.

With the help of image analysis techniques, the grey-scale histogram of the original image was used to distinguish the different phases. Within the grey-scale from 0 (black) to 256 (white), the pores, CSH gel, CH, limestone and unhydrated cement are identified respectively.

In order to make a quantitative comparison of the pore size distributions of the different samples a 2D backscatter image analysis technique was developed [15] and used in this study. The area of the feature (each individual subject) on the image of the polished surface was assessed by multiplying the number of pixels contained in the feature by the area per pixel. The diameter of an equivalent circle, equal in area to that of the feature, was calculated from which the cumulative pore area fraction against the equivalent pore diameter was obtained. In order to quantify the phases and the phase distribution, image analysis was performed on 10 samples of each mixture in order to obtain a 95% confidence interval for the true value [15].

2.6. Thermal analysis

Thermogravimetric analysis and derivative thermogravimetric analysis were performed on the samples at the age of 28 days, at atmospheric pressure in nitrogen (TA Instruments 2960 SDT V3.0 F, 10 °C/min, up to 1200 °C). Such techniques can be used to determine the phase composition in the cement paste.

3. Results and discussion

3.1. Rate of heat evolution during hydration

The heat evolution and the rate of heat evolution of the four mixtures are plotted in Fig. 2. Only the first 50 h of the rate of heat evolution are shown.

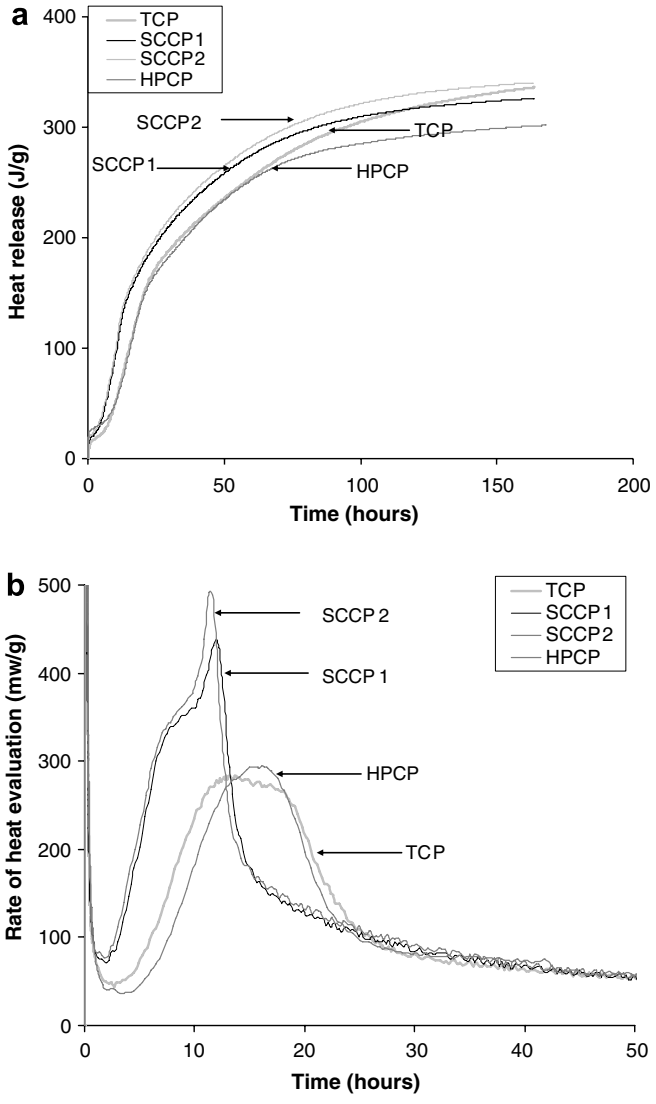

Fig. 2. (a) Heat release of pastes at 20 °C in the first 250 h and (b) rate of heat evolution of four different mixtures in the first 50 h at 20 °C.

The results clearly show that hydration is influenced by the presence of the limestone filler in the SCCP mixes. The differential curves of the heat production rate show three phenomena, namely a considerable shortening of the dormant stage, an acceleration of the hydration reactions during the acceleration period and the appearance of a third peak in the heat production rate at about 12 h.

To explain these phenomena two different hypotheses can be proposed. The first hypothesis states that the limestone filler is inert and therefore does not take part in the reactions during the hydration. On the one hand, it will figure as a nucleation core for the hydration of the C_3S and C_2S and shorten the dormant stage and accelerate the hydration reactions. On the other hand the presence of the filler will activate reactions that are not or less prominent present in a traditional concrete without limestone filler which results in the third peak in the curve of the heat production rate.

The second hypothesis does not consider the limestone filler to be inert, but sees it as an active partner in the hydration reactions. The appearance of a hydration peak after 12 h might then be explained by a conversion of ettringite to monocarbonate instead of monosulphate, which is a more stable compound and therefore results into a higher heat release.

Debates about these phenomena and the possible explanations are still going on [7,18,19].

Due to the faster heat release of SCCP containing limestone powder, the risk on early age thermal cracking might be somewhat higher. However, this has to be further investigated taking into account the development of mechanical properties during hydration.

3.2. Thermal analysis

The TGA curve can quantitatively provide the weight loss of each individual phase. Results on the thermal decomposition of four cement pastes are shown in Fig. 3.

For the interpretation of TGA and DTG results, most researchers [20–22] point out that:

(1) An extremum at 100–130 °C (TGA) corresponds with the evaporation of adsorbed water.
(2) Between 160 and 185 °C (DTG) a mass loss occurs defined here as hydrate water.
(3) Two or three low and broad maxima are on the DTG curve between 220 and 400 °C, corresponding to gel water release.
(4) A narrow and high trough occurs on both DTG and TGA curves at 450 °C, representing the decomposition of portlandite, $Ca(OH)_2 \rightarrow CaO + H_2O$ [20,23].
(5) Between 500 and 700 °C (TGA) a further dehydration and/or dehydroxylation occurs.
(6) Around 750 °C, a trough is found in the DTG curve. Correspondingly, a dramatic loss of mass was also observed from TGA, representing to the decomposition of calcite, $CaCO_3 \rightarrow CaO + CO_2$, with CO_2 escaping.

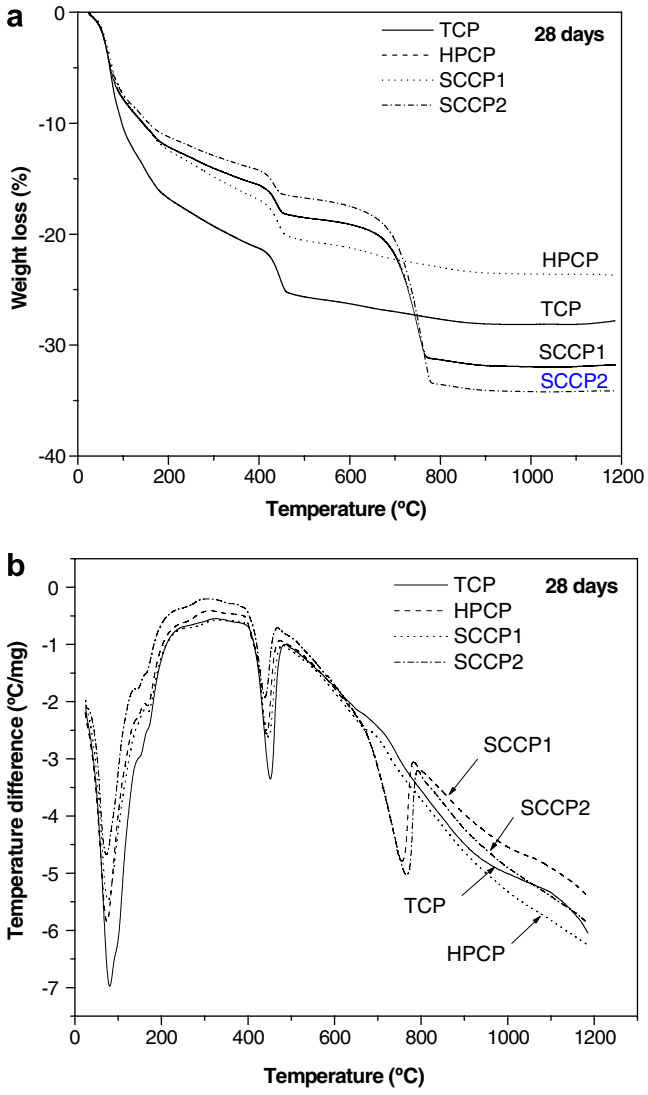

Fig. 3. (a) Thermal decomposition of pastes by thermogravimetric analysis (TGA) and (b) derivative thermogravimetric analysis (DTG).

When comparing the mass loss in the different mixtures, two main differences can be observed. Firstly, a much higher mass loss is found in TCP compared to SCCP and HPCP at 100–200 °C. This is due to the higher water content in the traditional concrete. Secondly, a bigger mass loss at 750 °C is observed only on the samples of SCCP1 and SCCP2.

The amount of CO_2 escaping from the cement paste can be calculated exactly from the TGA tests and compared with theoretical calculations. From Fig. 3, 10.29% and 13.25% of mass loss can be calculated for SCCP1 and

Table 3
Weight loss SCCP mixtures from TGA and theoretical calculations

	Weight loss from TGA (mg)	Weight loss from theoretical calculation (mg)
SCCP1	2.98	2.86
SCCP2	3.78	3.63

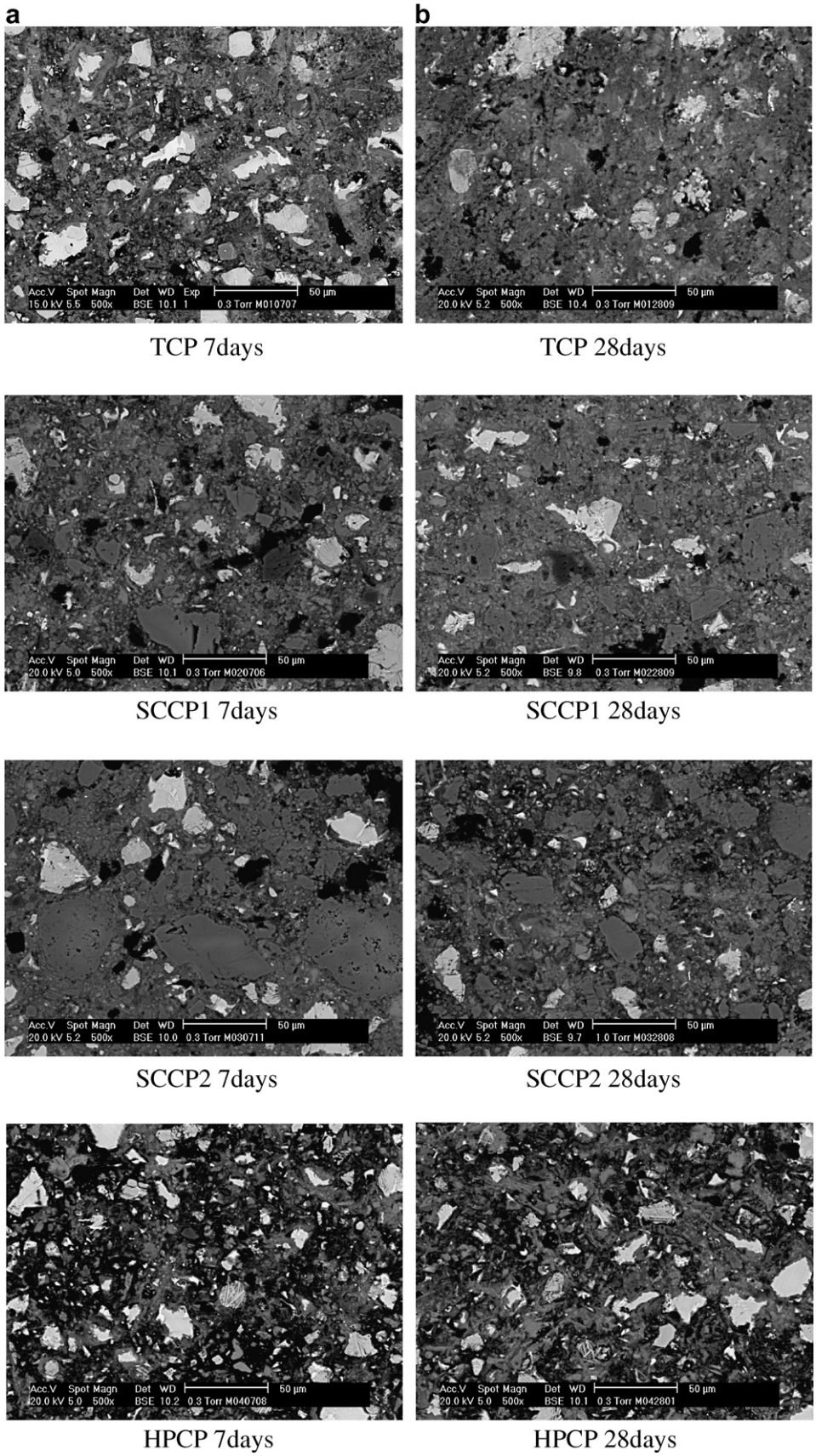

Fig. 4. BSE images of the pastes at age of 7 days (a) and 28 days (b).

Table 4
Phases distribution (in volume percentage) of mixtures at 3, 7 and 28 days

	Porosity (%)	CSH (%)	CH (%)	$CaCO_3$ (%)	Unhydrated cement (%)
TCP 3 days	21.73	35.55	24.56	–	18.26
SCCP1 3 days	13.00	36.74	19.40	15.65	15.30
SCCP2 3 days	15.39	32.44	22.61	16.37	13.19
HPCP 3 days	13.7	47.75	21.74	–	16.82
TCP 7 days	17.36	37.28	31.19	–	14.17
SCCP1 7 days	12.47	42.10	15.65	17.06	12.73
SCCP2 7 days	13.79	39.67	20.94	17.41	8.19
HPCP 7 days	11.44	50.04	26.42	–	12.10
TCP 28 days	14.26	48.40	27.32	–	10.02
SCCP1 28 days	9.32	46.07	21.20	16.94	6.47
SCCP2 28 days	11.96	42.13	22.36	17.37	6.18
HPCP 28 days	8.53	56.32	25.70	–	9.45

SCCP2 respectively. The total weight of the SCCP1 and SCCP2 samples was 28.9948 mg and 28.5063 mg respectively. The total amount of CO_2 escaping from the TG analysis is then 2.98 mg and 3.78 mg, respectively. Theoretically, according to the mass percentage of limestone in the mixture (Table 3), there is 7.54 mg and 9.56 mg $CaCO_3$ present in the sample of SCCP1 (28.9948 mg) and SCCP2 (28.5063 mg). The initial amount of CO_2 escaping from decomposition of carboniferous, $CaCO_3 \rightarrow CaO + CO_2$, should be 2.86 mg for SCCP1 and 3.63 mg for SCCP2.

Comparing the TGA analysis and the theoretical calculations, the weight loss measured with TGA is slightly higher than the weight loss from the theoretical calculations. If one takes into account that a small part of the weight losses is due to the decomposition of the calcium silicate hydrates in the cement paste, the main part of the weight loss at this temperature is due to decarbonation of the limestone. According to the mass balance law, it can be found that almost no limestone powder participated in the chemical reaction during cement hydration. The limestone powder acts only as inert filler in the SCCP (see also Section 3.1).

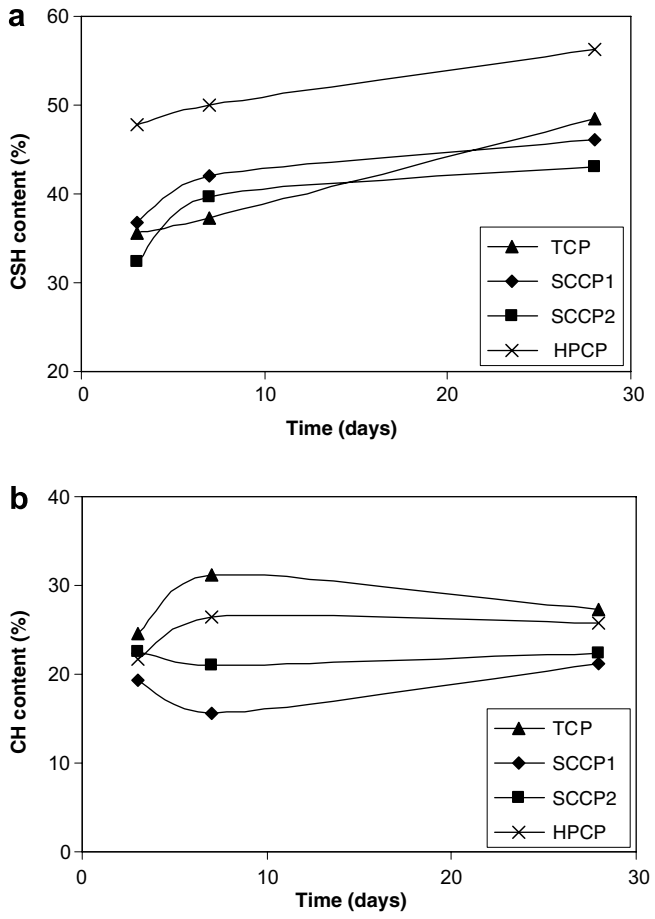

Fig. 5. (a) Development of the C–S–H phase and (b) CH phase.

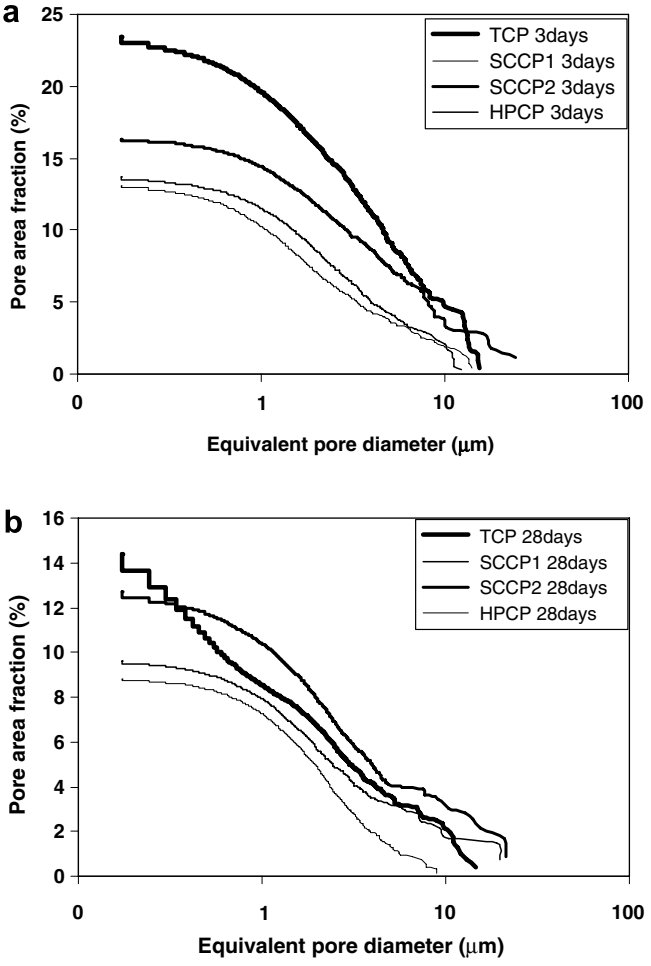

Fig. 6. Pore size distribution at curing ages of 3 days and 28 days.

3.3. Development of the microstructure

3.3.1. BSE observation

One of the BSE images from each mixture at the ages of 7 days and 28 days is shown in Fig. 4. Big pores can be found in both samples SCCP1 and SCCP2 at 7 days. These big pores are mainly situated around big limestone particles. It can also be seen that even very small limestone particles still exist in the pastes even after 28 days of hydration. Average results of 10 samples of each mixture at 3, 7 and 28 days on the phase distribution are listed in Table 4.

3.3.1.1. Solid phases. It is obvious that the unhydrated cement particles decrease with the increasing of curing age, which is shown in Table 4 for all mixtures. As can be seen in Fig. 5a, the development of CSH in the SCCP mixtures is similar in spite of their different w/c ratios. The HPCP shows higher CSH content due to the low w/c ratio. However, the development of CH is much different if SCCP is compared with HPCP and TCP. The CH content in SCCP decreases between 3 and 7 days and slightly increases afterwards. In HPCP and TCP, the CH content first increases until 7 days and decreases afterwards. This is consistent with the observations in [15]. The more water and ettringite are present, the more CH is converted into garnets.

3.3.1.2. Limestone powder. In SCCP samples, considering the accuracy obtained with the image analysis, the total amount of limestone powder is almost not changing during 28 days hydration (see Table 4). From the image analysis it is found that the interface between limestone and hydrates is quite porous, even in the samples having an age of 28 days. However, within the HPCP samples, the interface around the unhydrated cement is much denser.

3.3.1.3. Pore size distribution. The porosity decreases with the development of curing age for all mixtures. However, pore size and pore shape are significantly influenced by mix design. Fig. 6 shows the comparison of the four samples at 3 days (a) and 28 days (b). Significant differences are evident both in size and in shape of the pores. The 3-days old samples show higher porosity than the 28-days old samples. SCCP2 shows a very similar pore size distribution as HPCP. Of course the traditional cement paste has a much higher porosity than SCCP and HPCP both at the age of 3 days and 8 days.

3.3.2. Mercury intrusion porosimetry measurements

The pore size distribution measurements by MIP of two SCCP mixtures are shown in Fig. 7. The results at 3, 7, 28 and 56 days are plotted. Obviously, with the increase of the

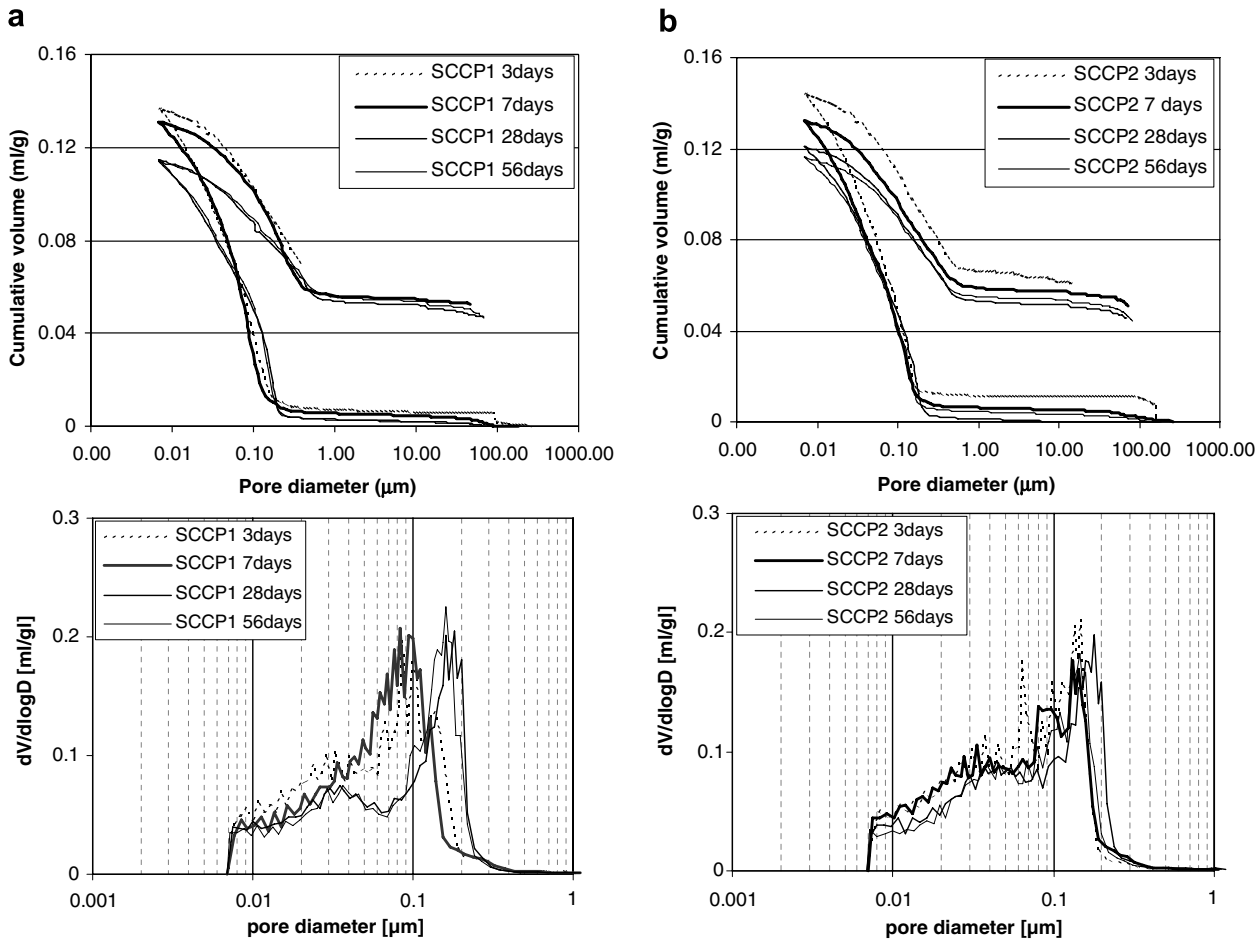

Fig. 7. Pore size distribution of the SCCP mixtures at different ages.

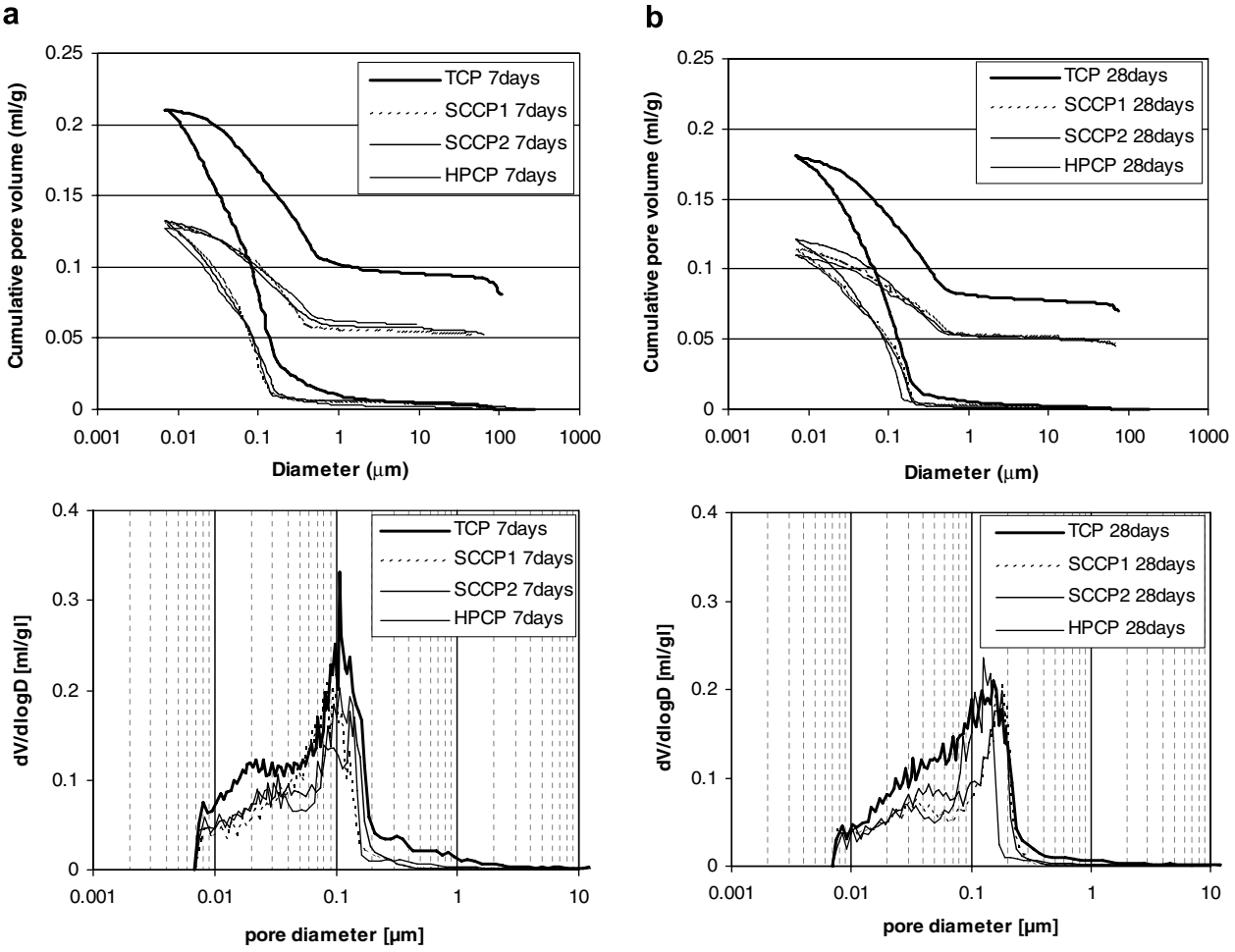

Fig. 8. Comparison of pore size distributions at 7 days and 28 days.

hydration time, the total porosity is decreasing, especially in the early hydration step. In the later stage, the changes in the total porosity are much slower than in the early ages. The critical pore diameters, defined as the peaks in the curves, giving the rate of mercury intrusion per change in pressure (differential curves) [12], did not show a significant change.

The comparison of the pore size distributions and the differential curves of pore size distribution of four mixtures at 7 days and 28 days are presented in Fig. 8. As expected, the total pore volume in traditional concrete is much higher than in SCCP and HPCP. However, there is only a slight difference of the total pore volume of SCCP and HPCP. This is consistent with BSE image analysis. The critical pore diameters of SCCP and HPCP samples are also almost the same as can be seen from Fig. 8.

4. Conclusions

In this study, the microstructure of self-compacting cement pastes is investigated in comparison to high performance cement paste and traditional cement paste. The following conclusions can be drawn:

1. The results of the heat evolution show that hydration is influenced by the presence of the limestone filler in the SCCP mixes The cumulative heat release in SCCP containing limestone powder is higher and the rate of heat release is also higher than for TCP and HPCP.
2. The development of the relative CH phases in SCCP is different from HPCP and TCP. The CH content in SCCP decreases till the curing age of 7 days and then increases.
3. Analysis both from BSE image analysis and MIP shows that the pore structure, including the total pore volume, pore size distribution and critical pore diameter, in the SCCP is very similar to that of HPCP.
4. The fact that limestone powder does not participate in the chemical reaction can be confirmed both from thermal analysis and BSE image analysis. However, limestone powder acts as an accelerator during early cement hydration.

Acknowledgements

The research was financially supported by the Fund for Scientific Research – Flanders (Belgium) (FWO), which is

gratefully acknowledged. The technical support during MIP measurements by the PMI (Porous Materials, Inc.) is also appreciated.

References

[1] Khayat KH, Hu C, Monty H. Stability of self-consolidating concrete, advantages, and potential applications. In: Wallevik O, Nielsson I, editors. First international RILEM symposium, SCC. Stockholm: RILEM Publications; 1999. p. 134–42.
[2] Skarendahl A, Petersson O, editors. Self-compacting concrete, state-of-the art report of RILEM Technical Committee 174-SCC, self-compacting concrete. RILEM Publications; 1999.
[3] Ozawa K, Maekawa K, Kunishima M, Okamura H. Development of high performance concrete based on the durability design of concrete structures. In: Okamura H, Shima H, editors. Second East-Asia and Pacific conference on structural engineering and construction, Kochi, Japan 1; 1988. p. 445–50.
[4] Okamura H, Ozawa K. Mix-design for self-compacting concrete. Concr Library, Jpn Soc Civil Eng (JSCE) 1995;25:107–20.
[5] Hayakawa M, Matsuoka Y, Shindoh T. Development and application of super workable concrete. In: Bartos PJ, editor. RILEM international workshop on special concretes: workability and mixing, Paisley: RILEM Publication; 1993. p. 183–90.
[6] Loukili A, Khelidj A, Richard P. Hydration kinetics, change of relative humidity, and autogenous shrinkage of ultra-high-strength concrete. Cem Concr Res 1999;29(4):577–84.
[7] Poppe AM. Influence of filler on hydration and properties of self-compacting concrete [In Dutch], Ph.D. thesis, Gent: University of Ghent; 2004.
[8] Okamura H, Ozawa K. Mix-design for self-compacting concrete. Concr Library Jpn Soc Civil Eng (JSCE) 1995;25:107–20.
[9] Billberg P. Mix design model for self-compacting concrete. First North American conference on the design and use of self-consolidating concrete, November 12–13. ACBM Publication; 2002. p. 65–70.
[10] Ambroise J, Péra J. Design of self-leveling concrete. First North American conference on the design and use of self-consolidating concrete, November 12–13. ACBM Publication; 2002. p. 93–8.
[11] Bager DH, Brandl M, Geiker MR, Thrane LN, Wallevik O. The effect of measuring procedure on the apparent rheological properties of self-compacting concrete. Cem Concr Res 2002;32(11):1791–5.
[12] Akkaya Y, Bui van K, Shah SP. Rheological model for self-consolidating concrete. ACI Mater J 2002;99(6):549–59.
[13] Petersson Ö. Investigation on workability of SCC: effects of aggregate size, additives and admixtures. Swedish Cement and Concrete Research Institute; 1999.
[14] Ferraris CF, Obla KH, Hill R. Influence of mineral admixtures on the rheology of cement paste and concrete. Cem Concr Res 2001;31(2):245–55.
[15] Ye G. Experimental study and numerical simulation of the development of the microstructure and permeability of cementitious materials. Ph.D. thesis. Delft: Delft University of Technology; 2003.
[16] Diamond S. Mercury porosimetry: an inappropriate method for the measurement of pore size distributions in cement-based materials. Cem Concr Res 2000;30(10):1517–25.
[17] Washburn EW. Proceedings of the national academy of sciences. PNASA; 1921. p. 7–21.
[18] Péra J, Husson S, Guilhot B. Influence of finely ground limestone on cement hydration. Cem Concr Comp 1999;21:99–105.
[19] Heikal M, El-Didamony H, Morsy MS. Limestone-filled pozzolanic cement. Cem Concr Res 2000;30:1827–34.
[20] Bazant ZP, Kaplan MF. Concrete at high temperatures. London: Longman-Addison-Wesley; 1996.
[21] Kakali G, Tsivilis S, Tsialtas A. Hydration of ordinary portland cements made from raw mix containing transition element oxides. Cem Concr Res 1998;28:335–40.
[22] Stepkowska ET, Blanes JM, Franco F, Real C, Pérez-Rodríguez JL. Phase transformation on heating of an aged cement paste. Thermochim Acta 2004;420(1–2):79–87.
[23] Buchler PM, Viera-coelho AC, Cartledge FK, Dweck J. Hydration of a portland cement blended with calcium carbonate. Thermochim Acta, 346. Irlanda: Belfast; 2000. p. 105–13.